Bendola Publishing
Journal of Transition Metal Complexes
Vol. 4 (2021), Article ID 236086, 7 pages
doi:10.32371/jtmc/236086

Research Article

Polynuclear 2D Copper(II) Complex of Pyrazine Containing Perchlorate As a Counter-Ion: Crystal Structure and DFT Calculations

Jorge S. Gancheff,[1] Florencia Luzardo,[1] Natalia Alvarez,[1] Karolina Soca Rosas,[1] Carlos Kremer,[1] and Andrea S. Stucchi de Camargo[2]

[1]*Área Química Inorgánica, Facultad de Química, Universidad de la República, 11800 Montevideo, Uruguay*
[2]*Physics Institute of São Carlos, University of São Paulo, São Carlos, SP 13566-590, Brazil*
Address correspondence to Jorge S. Gancheff, jorge@fq.edu.uy

Received 22 November 2019; Revised 4 December 2020; Accepted 27 January 2021

Abstract A new polynuclear cationic complex of copper(II) (Cu(II)) with pyrazine as a ligand and perchlorate acting as a counter-ion was obtained. X-ray diffraction results accounted for a 2D polymer array of cations, in which the metal-ions were located on an ideal square-pyramidal coordination environment defined by four nitrogen atoms of pyrazines and one chloride. The polymer compound, which extended along the *ab* plane of the structure, showed Cu(II) displaced 0.9 Å from the plane defined by the N-atoms and chloride. Perchlorate ions were situated in cavities interacting with pyrazine by anion-π weak interactions. These low-energy bonds emerged as a consequence of the π-acidity of pyrazine upon coordination to Cu(II). Density-functional theory (DFT) calculations at the M06-2X level of theory using 6-31G(d) and 6-31+G(d) were conducted aimed at achieving an electronic description of selected properties of title complex. M06-2X/6-31G(d), in particular, proved to be an acceptable performer in dealing with geometric aspects keeping the computational cost very low.

Keywords polymer compound; copper(II) complexes; pyrazine; DRX studies; DFT calculations

1. Introduction

Nitrogen heterocycles are ligands of paramount importance in coordination chemistry. Pyrazine (pyz), which is an N, N'-ditopic diimine, is not an exception and has been widely used for constructing many metal-organic frameworks containing several transition metal-ions [1,2,3,4,5,6,7]. With copper(II) (Cu(II)), in particular, pyrazine plays a remarkable role for building Cu coordination polymers. Interesting compounds have been observed [8,9,10,11,12,13], which are found in the distorted hexagonal ring $[Cu_6(CN)_2(pyz)_4]$ of the 3D-coordination polymer $^3_\infty[Cu_3(CN)_3 \cdot (pyz)_2]$; see [10] as an example. Polymer complexes of Cu(II) with pyrazine-containing ligands exhibit, in some cases, potential applications as gas storage system, chemical catalysis, and drug delivery, among others [14,15,16].

As a part of our interest to increase basic knowledge on structural properties of Cu(II) complexes containing diimine ligands, the synthesis and structure of a polymer array of Cu(II), pyrazine, and chloride containing perchlorate as a counter-ion are presented. The network extends along the *ab* plane of the structure, in which the metal-ion is observed slighty displaced from the plane defined by the N-donor atoms. Anions are hosted by the structure in cavities via noncovalent anion-π interaction involving coordinated pyrazine. To shed light into the electronic properties, geometry optimization and population analysis were performed with the density-functional theory (DFT) hybrid meta exchange-correlation functional M06-2X [17] combined with 6-31G(d) [18,19,20,21,22,23] and 6-31+G(d) [24].

2. Experimental

2.1. Materials and instrumentation

Reagents were obtained from major suppliers and used without further purifications. Elemental analyses for carbon, hydrogen, and nitrogen were performed on a Thermo Scientific Flash 2000 analyzer. FTIR spectra were recorded for the complex dispersed in KBr pellets on a Shimadzu IRPrestige-21 spectrometer.

2.2. Synthesis

A solution of 47 μL (0.60 mmol) of pyrazine in MeOH (8 mL) was carefully layered on top of an aqueous solution (8 mL) of Cu(II) chloride (51 mg, 0.30 mmol) and sodium perchlorate (74 mg, 0.60 mmol). Light-blue crystals were obtained after seven days (yield 47%). Anal. Calcd for $CuC_8H_8N_4O_4Cl_2$: C, 26.79; H, 2.25; N, 15.62. Found: C, 27.33; H, 2.08; N, 15.98. All values are given in percentage. FTIR (KBr, cm^{-1}): 3,130–3,110 (w, Csp^2-H), 1,427 (s, Ar), 1,105–1,075 (s, C−N).

2.3. Single-crystal X-ray diffraction study

Diffraction data were obtained at 293(2) K on a Bruker D8 Venture diffractometer equipped with a Photon 100 CMOS

Table 1: Selected crystallographic data, experimental details, and refinement results for $[CuCl(pyz)_2]_n(ClO_4)_n$.

Empirical formula	$C_8H_8Cl_2CuN_4O_4$
Formula weight	358.63
Temperature	293(2) K
Wavelength	1.54178 Å
Crystal system	Tetragonal
Space group	$P4/n$
Unit cell dimensions	$a = 9.7205(2)$ Å
	$b = 9.7205(2)$ Å
	$c = 5.9986(2)$ Å
	$\alpha = 90°$
	$\beta = 90°$
	$\gamma = 90°$
Volume	566.80(3) Å^3
Z	2
Density (calculated)	2.101 Mg m^{-3}
Absorption coefficient	7.263 mm^{-1}
$F(000)$	358
Crystal size	$0.103 \times 0.095 \times 0.082$ mm^3
Theta range for data collection	6.44–69.05°
Index ranges	$-9 \le h \le 11$, $-11 \le k \le 11$, $-3 \le l \le 7$
Reflections collected	2,338
Independent reflections	529 [R(int) = 0.0625]
Completeness to theta = 67.679°	99.2%
Absorption correction	Semiempirical from equivalents
Max. and min. transmission	0.58 and 0.48
Data/restraints/parameters	529/0/45
Goodness-of-fit on F^2	1.092
Final R indices [$I > 2$sigma(I)]	$R_1 = 0.0347$, $wR^2 = 0.0832$
R indices (all data)	$R_1 = 0.0448$, $wR^2 = 0.0885$
Largest diff. peak and hole	0.319 and -0.484 e Å^{-3}

detector with Cu-K_α radiation ($\lambda = 1.54178$ Å). APEX 3 software was used for data collection and reduction, and multiscan absorption correction was applied [25]. The structure was solved by iterative methods using SHELXT. Structure refinement was done using SHELXL-2018 [26, 27] within SHELXLE [28] by the full-matrix least squares on F2 method. Nonhydrogen atoms were refined using anisotropic displacement parameters, whereas hydrogen atoms were geometrically positioned and refined with the riding model. For carbon-bonded hydrogen-atoms, thermal parameters were set to 1.2 times the U_{eq} (equivalent isotropic displacement factor) of the carbon atom they are bonded to. The molecular graphics were prepared using MERCURY [29]. Selected crystallographic data, experimental details, and refinement results are summed up in Table 1.

2.4. Hirshfeld surface analysis

For the further understanding of the intermolecular interactions driving the hosting of perchlorate anion in the 2D polynuclear complex, the Hirshfeld surface around the anion was constructed. CRYSTAL EXPLORER17 was used to determine the surface [30,31], which was based on the CIF file. Normalized contact distances were mapped in the surface, where normalized contact distance (d_{norm}) is defined as

$$d_{\text{norm}} = \frac{d_i - r_i^{\text{vdW}}}{r_i^{\text{vdW}}} + \frac{d_e - r_e^{\text{vdW}}}{r_e^{\text{vdW}}},$$

where d_e and d_i represent the distances from a point on the surface to the nearest nucleus outside and inside the surface, respectively, and r^{vdW} corresponds to the van der Waals (vdW) radii of the atoms involved [32]. The bidirectional graph of d_e and d_i distances within the surface (and their frequency)—2D fingerprint plot—provided quantitative information about the type of interactions [33].

2.5. Theoretical calculations

All calculations were conducted at the DFT. Geometry optimizations starting from molecular structure determined by X-ray diffraction were carried out. In all cases, M06-2X [17] in combination with 6-31G(d) [18,19, 20,21,22,23] was used, and an ultrafine grid featured by 90 radial shells and 590 angular points per shell was considered. Diffuse functions were also taken into account (by using 6-31+G(d) [24]) aimed at inferring the influence of counter-ions on electronic properties. Thus, the system $[CuCl(pyz)_4]^+\cdots ClO_4^-$ was studied by using M06-2X in combination with 6-31+G(d) in the gas phase. To explore how pyrazine (as a bridging-ligand) affects electronic properties, the model complex $\{CuCl(\mu\text{-pyz})_4[CuCl(NH_3)_3]_4\}^{5+}$ was considered, in which pyrazine of terminal units was substituted by NH_3. Any attempts to optimize the geometry of this model complex with M06-2X/6-31G(d),6-31+G(d) were unsuccessful. Thus, we decide to consider a diamagnetic substitution approach in the model complex by replacing all Cu(II)-terminal cationic units by the neutral ones $\{ZnCl_2(H_2O)_3\}$. This approach led to the new model complex $\{CuCl(\mu\text{-pyz})_4[ZnCl_2(H_2O)_3]_4\}^+$, whose geometry was optimized with M062X/6-31G(d) (further details are in Section 3.3). The nature of the stationary point was verified through vibrational analysis (no imaginary frequencies at the minimum). Natural population analysis (NPA) calculations were performed with the NBO code [34, 35,36,37] included in the program package GAUSSIAN09, Rev. D01 [38], which was used for all theoretical studies reported in this contribution.

3. Results and discussion

3.1. Crystal structure

The reaction of pyrazine in the presence of Cu(II), chloride, and perchlorate in MeOH:H_2O (1:1; v:v) led to the formation of a new 2D array of cation in complex

Table 2: Selected bond lengths (Å) and angles (°).

Bond length	
N(1)–Cu(01)	2.056(2)
Cu(01)–Cl(3)	2.547(2)
Bond angle	
N(1)–Cu(01)–N(1)#2	169.85(15)
N(1)–Cu(01)–N(1)#3	89.552(14)
N(1)–Cu(01)–Cl(3)	95.07(8)

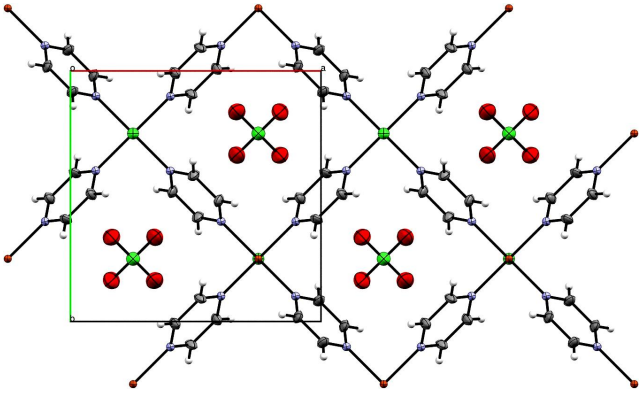

Figure 1: 2D array of the title complex (perspective view along the c-axis). Thermal ellipsoids are drawn at the 50% probability level.

$[CuCl(pyz)_2]_n(ClO_4)_n$. The mononuclear subunit shows the metal-ion seated on an ideal square-pyramidal coordination environment [39,40], in which Cu(II) is bonded to a chloride and to four nitrogen atoms of the pyrazine-ligand with distances of 2.547(2) and 2.052(2) Å, respectively. Selected inequivalent bond lengths and angles are presented in Table 2; bond lengths and angles generated by symmetry and otherwise equivalent to the ones presented are excluded for clarity. It deserves to be mentioned that distance Cu−N was in line with the one observed in complexes of Cu(II) with pyrazine-containing ligands [41,42]. In this regard, complexes of Cu(II) with pyridylalkylamide ligands *N*-(pyridin-2-ylmethyl)pyrazine-2-carboxamide and *N*-(2-(pyridin-2-yl)ethyl)pyrazine-2-carboxamide, taken as an example into account, exhibit Cu−N bond distances in the range from 1.997 Å to 2.067 Å [41].

The polymer array extends along the *ab* plane of the structure (Figure 1), in which the metal-ion is observed displaced 0.9 Å from the plane defined by the N-donor atoms, and chloride appears apically coordinated in an alternate fashion (Figure 2).

The sequence {Cu(II)-pyz-Cu(II)-pyz-Cu(II)} runs along the *[220]* and *[110]* directions, with pyrazine-ligands being observed tilted to each other. Polarization of the π-electron density induced by coordination to metal-ions is typical for pyrazine in the role of bridging-ligand [43],

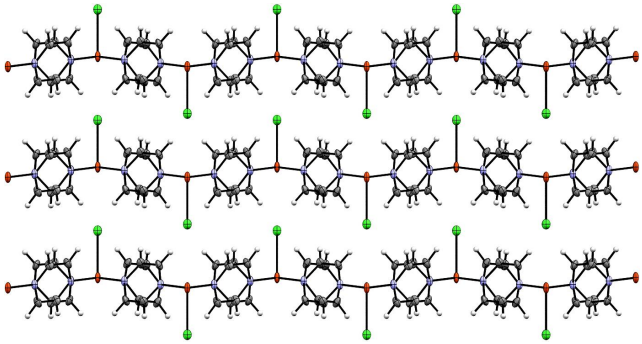

Figure 2: Alternate orientation of chloride in the *bc* plane (perchlorate anions have been omitted for clarity).

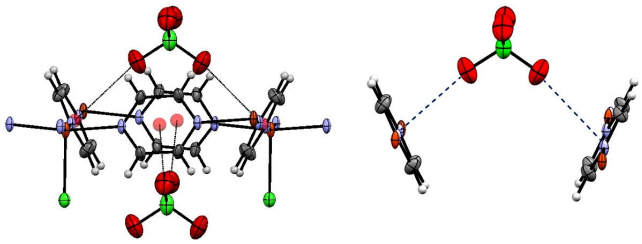

Figure 3: Partial views of the interaction of ClO_4^- with the centroid of the aromatic rings of pyrazines.

which points this ligand to present an important π-acidity in the title complex. Thus, this π-acidity is expected to prevail in the interior of all cavities (i.e., voids which were obtained upon the formation of the polynuclear 2D crystal structure) in which perchlorate ions are located. Consequently, anion-π weak interactions emerge and perchlorate ions appear connected to pyrazine (aided by the tilted orientation of this ligand) (Figure 3). Distance $O_3Cl{-}O\cdots$pyz (centroid) of 3.146 Å is observed, and this metric parameter appears in line with the ones observed in related systems [44,45,46].

3.2. Hirshfeld surface analysis

In order to better understand the position of the perchlorate anion in the lattice, and how it functioned as a template for the construction of the 2D polynuclear complex, a Hirshfeld surface was constructed around it. The d_{norm} mapped through the surface confirms that the predominant intermolecular interaction with the 2D polynuclear complex is anion-π interactions (Figure 4). These are sufficiently strong to generate red hotspots throughout the surface, where the interatomic distance is significantly shorter than the sum of the van der Waals radii of the atoms indicating the existence of a bond-type interaction. The largest hotspots are surrounding the O atoms on the side oriented towards the adjacent pyrazine ligand. Moreover, when the 2D fingerprint (Figure 4) is calculated, the most frequent interactions (painted green and red in the fingerprint plot)

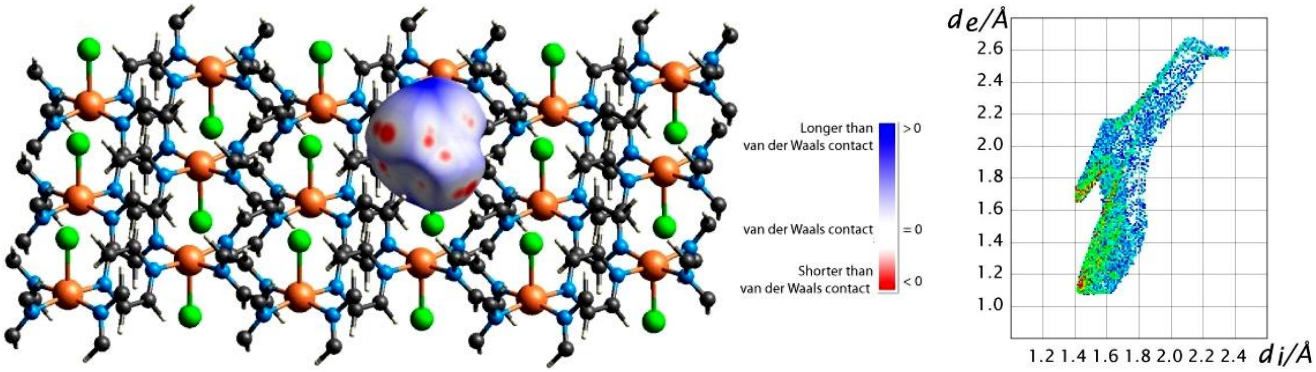

(a) (b)

Figure 4: Hirshfeld surface of one perchlorate on the 2D array of copper, pyrazine, and chloride (a), and resulting 2D-fingerprint plot (b).

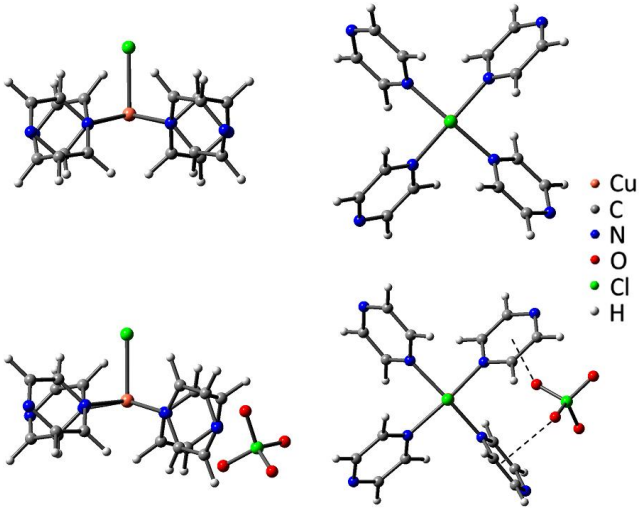

Figure 5: Optimized geometry of $[CuCl(pyz)_4]^+$ (top) and of $[CuCl(pyz)_4]^+ \cdots ClO_4^-$ (bottom) as obtained with M06-2X/6-31+G(d) in the gas phase ($T = 298\,K$). Anion-π interactions in dashed line.

correspond to atom-atom distances between 2.0 Å and 3.2 Å, corresponding to Cl−O···H Cl−O···C contacts in the Cl−O···pyz interaction.

3.3. Geometry optimization and NPA results

Results from X-ray diffraction measurements account for a 2D-array of Cu(II), chloride, and pyrazine having perchlorate as a counter-ion, which is observed hosted in cavities interacting with the aromatic units by anion-π interactions. Thus, we decided to optimize one model complex $[CuCl(pyz)_4]^+$, and the system $[CuCl(pyz)_4]^+ \cdots ClO_4^-$ (Figure 5) with M06-2X/6-31+G(d) to shed light into the influence of noncovalent interactions on geometric parameters and population analysis. A minimum as a stationary point was obtained for both geometry optimizations. Equilibrium geometry of complex (Figure 5) shows the metal atom in an ideal square-pyramidal environment, and these results are in accordance with the experimental results. Distances Cu−N (of 2.100 Å) resulted overestimated by +0.044 Å, while the one of bond Cu−Cl (of 2.363 Å) resulted underestimated by −0.184 Å. The presence of perchlorate induces the heterocycles to twist in order to promote anion-π interactions, with results being in line with those detected in the solid state. Additionally, an improvement of the Cu−N metric parameter of interacting pyrazine-ligands is obtained with a very good match with respect to the experimental finding (deviation of −0.002 Å), with improvement being not observed in this extension for Cu−Cl distance (difference of −0.158 Å) (Table 3).

Population analysis for $[CuCl(pyz)_4]^+$ obtained with M06-2X/6-31+G(d) shows the metal center carrying a charge of +1.021, which is markedly smaller than the formal charge of +2 as a result of a donation process, in which chloride ends with a charge of −0.665. While pyrazine shows a natural charge of −0.421 on nitrogen atoms, its coordination induces a polarization in the π-system as indicated by the charge of −0.519 on coordinated nitrogen atoms, and of −0.372 on the uncoordinated donor atoms.

Changes are observed by the inclusion of counter-ion in system $[CuCl(pyz)_4]^+ \cdots ClO_4^-$. While copper appears as $Cu^{+1.036}$, NPA results for nitrogen seems to be dependent on position and role of this donor atom. Population results for coordinated nitrogen of pyrazines interacting with ClO_4^- are of −0.536, with the charge of those donor atoms in opposite position being of −0.376. The presence of noncovalent anion-π interactions also affects the natural charge of all atoms on noninteracting pyrazine. Coordinated nitrogen appears with a charge of −0.499, with the ones remaining uncoordinated ending with a charge of −0.388.

Table 3: Selected optimized parameters (bond lengths in Å, bond angles in °) of $[CuCl(pyz)_4]^+$, $[CuCl(pyz)_4]^+\cdots ClO_4^-$, and $\{CuCl(\mu\text{-pyz})_4[ZnCl_2(H_2O)_3]_4\}^+$ as obtained with M06-2X/6-31+G(d), 6-31G(d) in the gas phase ($T = 298$ K).

System	Cu-pyz-631+d[1]	Cu-ClO_4-631+d[2]	Cu-pyz-631d[3]	Cu-Zn-631d[4]
		Bond lengths		
Cu−N	2.100	2.136, 2.139, 2.056[6]	2.079	2.077, 2.080, 2.081
Cu−Cl	2.363	2.388	2.349	2.340
N−C	1.339, 1.332[5]	1.349[7], 1.329[5]	1.339, 1.331[5]	1.338
N···N	2.783	2.785	2.783	2.759 (avg)
System	Cu-pyz-631+d	Cu-ClO_4-631+d	Cu-pyz-631d	Cu-Zn-631d
		Bond angles		
N−Cu−N	88.6	91.4, 86.8[6]	88.2	87.7, 88.2
N−Cu−Cl	98.8	95.4[6], 102.2, 104.4	100.0	100.3, 100.5, 100.8
Cu−N−C	117.7, 124.4	117.26[6], 118.6	17.4, 124.9	117.3, 124.2 (avg)
C−N−C	117.8, 116.8[5]	124.9[6], 124.0, 122.8	117.7, 116.8[5]	118.2, 188.8[7]

[1]Cu-pyz-631+d = $[CuCl(pyz)_4]^+$/M06-2X/6-31+G(d); [2]Cu-ClO_4-631+d = $[CuCl(pyz)_4]^+\cdots ClO_4^-$/M06-2X/6-31+G(d); [3]Cu-pyz-631d = $[CuCl(pyz)_4]^+$/M06-2X/6-31G(d); [4]Cu-Zn-631d = $\{CuCl(\mu\text{-pyz})_4[ZnCl_2(H_2O)_3]_4\}^+$/M06-2X/6-31G(d); [5]Average value involving noncoordinated nitrogen atoms; [6]Nitrogen in opposition to ClO_4^-; [7]Nitrogen coordinated to Zn(II).

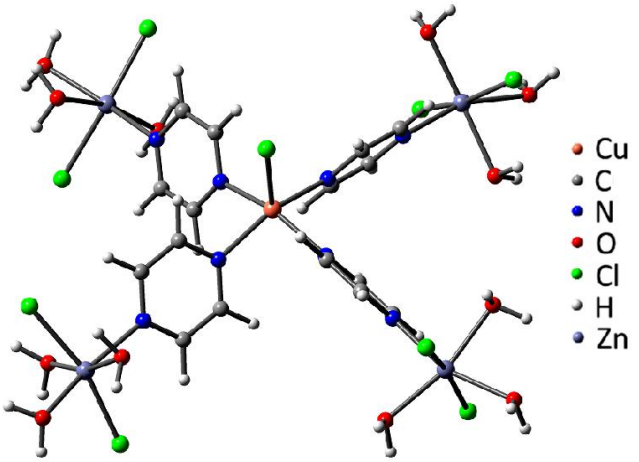

Figure 6: Optimized geometry of $\{CuCl(\mu\text{-pyz})_4[ZnCl_2(H_2O)_3]_4\}^+$ as obtained with M06-2X/6-31G(d) in the gas phase ($T = 298$ K).

The influence of pyrazine as a bridging-ligand on metric parameters was explored by comparing $[CuCl(pyz)_4]^+$ with the model complex $\{CuCl(\mu\text{-pyz})_4[ZnCl_2(H_2O)_3]_4\}^+$. Optimized geometry of the polynuclear model complex is displayed in Figure 6, and cartesian coordinates of the mononuclear one are included in the Supplementary Material (Table S1).

In going from the mononuclear complex to the model system, no important changes in geometric parameters are detected. Distances Cu−Cl and Cu−N of 2.349 Å and 2.079 Å, respectively, are observed in $[CuCl(pyz)_4]^+$, with these parameters remaining practically unchanged upon coordination of pyrazine to Zn(II) (d(Cu−Cl) = 2.341 Å; d(Cu−N) = 2.077–2.081 Å). As in the case of 6-31+G(d), the computational nonexpensive 6-31G(d) basis set accounts for an underestimation of Cu−Cl distance with respect to the experimental results (deviation of −0.198 Å), while an overestimation but reasonable match is obtained in Cu−N distance (deviation of +0.027 Å).

Population analysis of selected atoms in $\{CuCl(\mu\text{-pyz})_4[ZnCl_2(H_2O)_3]_4\}^+$ was also conducted. In this regard, NPA results of pyrazine seems to show dependence on metal ion. While nitrogen atoms bonded to Cu(II) display a charge of −0.541, the ones coordinated to Zn(II) exhibit a charge of −0.464. The coordination process promotes Cu(II) to carry a charge of +1.162 and chloride ends as $Cl^{-0.689}$, with both results being practically identical to the ones observed in mononuclear system.

4. Concluding remarks

A new bidimensional array of Cu(II), pyrazine, chloride, and perchlorate as a counter-ion was obtained in the solid state. X-ray diffraction results exhibited the metal-center seated on an ideal square-pyramidal coordination environment given by four N-donor atoms and chloride, which appears apically coordinated. Pyrazine was observed tilted to each other along the structure, and this relative orientation promoted this ligand to participate in noncovalent anion-π weak interactions with perchlorate. This anion was located in cavities obtained upon formation of the 2D polymer array, in whose interior is expected to prevail the effects of the π-acidity displayed by coordinated pyrazine.

Theoretical studies at the DFT theory were conducted using M06-2X in combination with 6-31G(d), and diffuse functions were added (through 6-31+G(d)) to explore the influence of counter-ions in geometry and population analysis. The effect on geometric parameters of pyrazine as bridging-ligand was explored—taken M06-2X/6-31G(d) into account—by comparing $[CuCl(pyz)_4]^+$ with a system, in which pyrazine connects Cu(II) to diamagnetic and neutral units $\{ZnCl_2(H_2O)_3\}$.

The presence of ClO_4^- induced a twist of the aromatic ring of pyrazine in order to promote the anion-π interactions experimentally observed. Even when the inclusion of counter-ion and diffuse function seemed to be necessary to get a good description of equilibrium geometry, M06-2X/6-31G(d), applied to the simple $[CuCl(pyz)_4]^+$ complex, proved to be an acceptable performer in dealing with geometric aspects keeping the computational cost very low. This conclusion also emerged for those systems in which pyrazine acts as bridging-ligand.

Finally, we hope that our work contributes with new elements to the design of coordination polymers of interest, and to the study of the packing forces responsible of the solid state structure.

Supplementary material Crystallographic data for the structural analysis have been deposited with the Cambridge Crystallographic Data Centre (CCDC) reference number 1961006. A copy of this information may be obtained via http://www.ccdc.cam.ac.uk, or from the Cambridge Crystallographic Data Centre, 12 Union Road, Cambridge CB2 1EZ, UK; fax: (+44) 1223-336-033, or e-mail: deposit@ccdc.cam.ac.uk.

Coordinates (x, y, z) of optimized systems in the gas phase employing M06-2X in combination with different basis sets at $T = 298$ K.

Conflict of interest The authors declare that they have no conflict of interest.

References

[1] P. M. Bhatt, Y. Belmabkhout, A. Cadiau, K. Adil, O. Shekhah, A. Shkurenko, et al., *A fine-tuned fluorinated MOF addresses the needs for trace CO_2 removal and air capture using physisorption*, J Am Chem Soc, 138 (2016), 9301–9307.

[2] P. Kanoo, S. K. Reddy, G. Kumari, R. Haldar, C. Narayana, S. Balasubramanian, et al., *Unusual room temperature CO_2 uptake in a fluoro-functionalized MOF: insight from Raman spectroscopy and theoretical studies*, Chem Commun (Camb), 48 (2012), 8487–8489.

[3] P. J. Steel and C. M. Fitchett, *Metallosupramolecular silver(I) assemblies based on pyrazine and related ligands*, Coord Chem Rev, 252 (2008), 990–1006.

[4] W.-G. Lu, J.-Z. Gu, L. Jiang, M.-Y. Tan, and T.-B. Lu, *Achiral and chiral coordination polymers containing helical chains: the chirality transfer between helical chains*, Cryst Growth Des, 8 (2008), 192–199.

[5] G. Bhosekar, I. Jess, and C. Näther, *On the preparation of coordination polymers by controlled thermal decomposition: synthesis, crystal structures, and thermal properties of zinc halide pyrazine coordination compounds*, Inorg Chem, 45 (2006), 6508–6515.

[6] X. Hao, Y. Wei, and S. Zhang, *Crystal structure and metamagnetic property of a 2-D layered complex, $[Fe^{II}(N_3)_2(pyz)]_n$ (pyz = pyrazine)*, Chem Commun, 2000 (2000), 2271–2272.

[7] S. Kitagawa, T. Okubo, S. Kawata, M. Kondo, M. Katada, and H. Kobayashi, *An oxalate-linked copper(II) coordination polymer, $[Cu_2(oxalate)_2(pyrazine)_3]_n$, constructed with two different copper units: x-ray crystallographic and electronic structures*, Inorg Chem, 34 (1995), 4790–4796.

[8] M.-L. Qi, K. Yu, Z.-H. Su, C.-X. Wang, C.-M. Wang, B.-B. Zhou, et al., *Three new three-dimensional organic-inorganic hybrid compounds based on $PMo_{12}O_{40}^{n-}$ ($n = 3$ or 4) polyanions and Cu^I-pyrazine/Cu^I-pyrazine-Cl porous coordination polymers*, Dalton Trans, 42 (2013), 7586–7594.

[9] I. Malaestean, V. Kravtsov, J. Lipkowski, E. Cariati, S. Righetto, D. Marinotto, et al., *Partial in situ reduction of copper(II) resulting in one-pot formation of 2D neutral and 3D cationic copper(I) iodide-pyrazine coordination polymers: structure and emissive properties*, Inorg Chem, 56 (2017), 5141–5151.

[10] S. E. H. Etaiw and S. N. Abdou, *Structure and spectral properties of pyrazine ligand assisted self-assembly of a coordination polymer containing copper-cyanide building blocks*, J Inorg Organomet Polym Mater, 23 (2013), 1296–1304.

[11] J. L. Manson, T. Lancaster, J. A. Schlueter, S. J. Blundell, M. L. Brooks, F. L. Pratt, et al., *Characterization of the crystal and magnetic structures of the mixed-anion coordination polymer $Cu(HCO_2)(NO_3)(pyz)$ {pyz = Pyrazine} by X-ray diffraction, ac magnetic susceptibility, dc magnetization, muon-spin relaxation, and spin dimer analysis*, Inorg Chem, 46 (2007), 213–220.

[12] T. F. Liu, H. L. Sun, S. Gao, S. W. Zhang, and T. C. Lau, *Ferromagnetic ordering and metamagnetism in malonate bridged 3D diamond-like and honeycomb-like networks: $[Cu(mal)(DMF)]_n$ and $\{[Cu(mal)(0.5pyz)]\cdot H_2O\}_n$ (mal = malonate dianion, DMF = N,N-dimethylformamide, pyz = pyrazine)*, Inorg Chem, 42 (2003), 4792–4794.

[13] Y. Rodríguez-Martín, M. Hernández-Molina, F. S. Delgado, J. Pasán, C. Ruiz-Pérez, J. Sanchiz, et al., *The flexibility of molecular components as a suitable tool in designing extended magnetic systems*, CrystEngComm, 4 (2002), 440–446.

[14] Z.-F. He and X.-H. Sun, *Structural diversity and anticancer activity on human myocardial aneurysm cells of two Cu(II)-coordination polymers*, Main Group Chem, 19 (2020), 81–89.

[15] M. Bonneau, C. Lavenn, P. Ginet, K. Otake, and S. Kitagawa, *Upscale synthesis of a binary pillared layered MOF for hydrocarbon gas storage and separation*, Green Chem, 22 (2020), 718–724.

[16] M. Sutradhar, T. Roy Barman, E. C. B. A. Alegria, M. F. C. Guedes da Silva, C. M. Liu, H. Z. Kou, et al., *Cu(II) complexes of N-rich aroylhydrazone: magnetism and catalytic activity towards microwave-assisted oxidation of xylenes*, Dalton Trans, 48 (2019), 12839–12849.

[17] Y. Zhao and D. G. Truhlar, *The M06 suite of density functionals for main group thermochemistry, thermochemical kinetics, noncovalent interactions, excited states, and transition elements: two new functionals and systematic testing of four M06-class functionals and 12 other functionals*, Theor Chem Acc, 120 (2008), 215–241.

[18] P. C. Hariharan and J. A. Pople, *The influence of polarization functions on molecular orbital hydrogenation energies*, Theor Chim Acta, 28 (1973), 213–222.

[19] M. M. Francl, W. J. Pietro, W. J. Hehre, J. S. Binkley, M. S. Gordon, D. J. DeFrees, et al., *Self-consistent molecular orbital methods. XXIII. A polarization-type basis set for second-row elements*, J Chem Phys, 77 (1982), 3654–3665.

[20] V. Rassolov, J. Pople, M. Ratner, and T. Windus, *6-31G* basis set for atoms K through Zn*, J Chem Phys, 109 (1998), 1223–1229.

[21] N. B. Balabanov and K. A. Peterson, *Systematically convergent basis sets for transition metals. I. All-electron correlation consistent basis sets for the 3d elements Sc-Zn*, J Chem Phys, 123 (2005), 064107–1–064107–15.

[22] D. Feller, *The role of databases in support of computational chemistry calculations*, J Comput Chem, 17 (1996), 1571–1586.

[23] K. L. Schuchardt, B. T. Didier, T. Elsethagen, L. Sun, V. Gurumoorthi, J. Chase, et al., *Basis set exchange: a community database for computational sciences*, J Chem Inf Model, 47 (2007), 1045–1052.

[24] G. W. Spitznagel, T. Clark, P. von Ragué Schleyer, and W. J. Hehre, *An evaluation of the performance of diffuse function-augmented basis sets for second row elements, Na-Cl*, J Comput Chem, 8 (1987), 1109–1116.

[25] R. H. Blessing, *An empirical correction for absorption anisotropy*, Acta Crystallogr A, 51 (1995), 33–38.
[26] G. M. Sheldrick, *A short history of SHELX*, Acta Crystallogr A, 64 (2008), 112–122.
[27] G. M. Sheldrick, *Crystal structure refinement with SHELXL*, Acta Crystallogr C Struct Chem, 71 (2015), 3–8.
[28] C. B. Hübschle, G. M. Sheldrick, and B. Dittrich, *ShelXle: a Qt graphical user interface for SHELXL*, J Appl Crystallogr, 44 (2011), 1281–1284.
[29] P. R. Edgington, P. McCabe, C. F. Macrae, E. Pidcock, G. P. Shields, R. Taylor, et al., *Mercury: visualization and analysis of crystal structures*, J Appl Crystallogr, 39 (2006), 453–457.
[30] S. Wolff, D. Grimwood, J. McKinnon, M. Turner, D. Jayatilaka, and M. Spackman, *CrystalExplorer (Version 3.1)*, University of Western Australia, 2012.
[31] A. Edwards, C. Mackenzie, P. Spackman, D. Jayatilaka, and M. Spackman, *Intermolecular interactions in molecular crystals: what's in a name?*, Faraday Discuss, 203 (2017), 93–112.
[32] M. A. Spackman and D. Jayatilaka, *Hirshfeld surface analysis*, CrystEngComm, 11 (2009), 19–32.
[33] J. J. McKinnon, D. Jayatilaka, and M. A. Spackman, *Towards quantitative analysis of intermolecular interactions with Hirshfeld surfaces*, Chem Commun, 2007 (2007), 3814–3816.
[34] J. P. Foster and F. Weinhold, *Natural hybrid orbitals*, J Am Chem Soc, 102 (1980), 7211–7218.
[35] A. E. Reed and F. Weinhold, *Natural localized molecular orbitals*, J Chem Phys, 83 (1985), 1736–1740.
[36] A. E. Reed, R. B. Weinstock, and F. Weinhold, *Natural population analysis*, J Chem Phys, 83 (1985), 735–746.
[37] A. E. Reed, L. A. Curtiss, and F. Weinhold, *Intermolecular interactions from a natural bond orbital, donor-acceptor viewpoint*, Chem Rev, 88 (1988), 899–926.
[38] M. J. Frisch, H. B. Schlegel, G. E. Scuseria, M. A. Robb, J. R. Cheeseman, G. Scalmani, et al., *Gaussian 09, Revision D.01*, Gaussian, Inc., Wallingford CT, 2009.
[39] S. Alvarez and M. Llunell, *Continuous symmetry measures of penta-coordinate molecules: Berry and non-Berry distortions of the trigonal bipyramid*, J Chem Soc Dalton Trans, 2000 (2000), 3288–3303.
[40] M. Llunell, D. Casanova, J. Cirera, P. Alemany, and S. Alvarez, *SHAPE, Version 1.21*, 2003.
[41] R. P. Houser, Z. Wang, D. R. Powell, and T. J. Hubin, *Copper(I) and copper(II) complexes with pyrazine-containing pyridylalkylamide ligands N-(pyridin-2-ylmethyl)pyrazine-2-carboxamide and N-(2-(pyridin-2-yl)ethyl)pyrazine-2-carboxamide*, Journal of Coordination Chemistry, 66 (2013), 4080–4092.
[42] R. H. Ismayilov, W. Z. Wang, G. H. Lee, and S. M. Peng, *One-, two- and three-dimensional Cu(II) complexes built via new oligopyrazinediamine ligands: from antiferromagnetic to ferromagnetic coupling*, Dalton Trans, 2006 (2006), 478–491.
[43] D. Quiñonero, A. Frontera, and P. M. Deyà, *High-level ab initio study of anion-π interactions in pyridine and pyrazine rings coordinated to Ag^I*, Chemphyschem, 9 (2008), 397–399.
[44] C. A. Black, L. R. Hanton, and M. D. Spicer, *Probing anion-π interactions in 1-D Co(II), Ni(II), and Cd(II) coordination polymers containing flexible pyrazine ligands*, Inorg Chem, 46 (2007), 3669–3679.
[45] C. A. Black, L. R. Hanton, and M. D. Spicer, *A coordination polymer strategy for anion encapsulation: anion-π interactions in (4,4) nets formed from Ag(I) salts and a flexible pyrimidine ligand*, Chem Commun, 2007 (2007), 3171–3171.
[46] K. V. Domasevitch, P. V. Solntsev, I. A. Gural'skiy, H. Krautscheid, E. B. Rusanov, A. N. Chernega, et al., *Silver(I) ions bridged by pyridazine: doubling the ligand functionality for the design of unusual 3D coordination frameworks*, Dalton Trans, 2007 (2007), 3893–3905.